Faraday Discussions

Accepted Manuscript

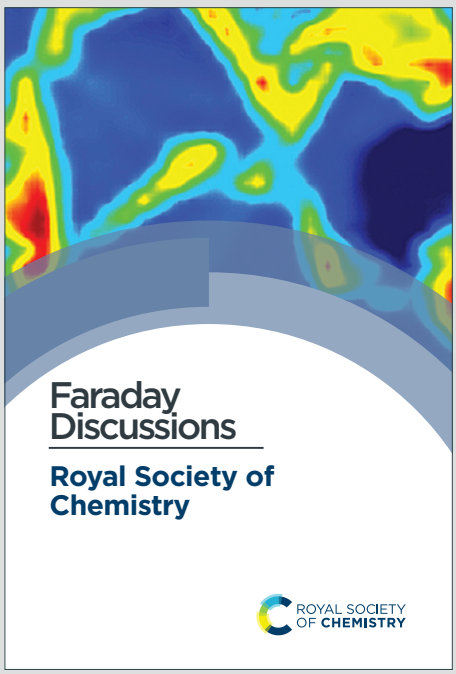

This article can be cited before page numbers have been issued, to do this please use: Y. Wang, N. An, B. Huang and Y. Zhai, *Faraday Discuss.*, 2024, DOI: 10.1039/D4FD00117F.

ROYAL SOCIETY OF CHEMISTRY

www.rsc.org/faraday_d

Non-sticky SiN_x nanonets for single protein denaturation analysis

View Article Online
DOI: 10.1039/D4FD00117F

Yuanhao Wang[a], Nan An[a], Bintong Huang[a, b*], and Yueming Zhai[a*]

[a] *The Institute for Advanced Studies (IAS), Wuhan University, Wuhan, 430072, P. R. China.*

[b] *School of Physics and Technology, Wuhan University, Wuhan 430072, Hubei, China.*

Email: bthuang@whu.edu.cn; yueming@whu.edu.cn

Abstract: Proteins play crucial roles in nearly all biological activities, with their functional structures deriving from stable folded conformations. Protein denaturation, induced by chemical and physical agents, is a complex process where proteins lose their stable structures, thereby impairing their biological functions. Characterizing protein denaturation at the single-molecule level remains a significant challenge. In this study, we developed non-adhesive silicon nitride nanonets coated with polyethylene glycol to capture individual proteins. We utilized these nanonets to investigate the denaturation of ovalbumin induced by guanidine hydrochloride (Gdn-HCl) and lead chloride. The entire denaturation and renaturation processes of a single ovalbumin molecule were monitored via ionic current measurements through the nanonets. These non-sticky nanonets offer a versatile tool for real-time studies of structural changes during protein denaturation.

Introduction

Protein denaturation refers to the structural alteration of proteins that leads to the loss of their biological function. When proteins are exposed to external stressors such as changes in temperature, pH, chemical exposure, or mechanical agitation, these delicate interactions can be disrupted, causing the protein to unfold or misfold. Understanding protein denaturation is critical across multiple fields. In biochemistry and molecular biology, it provides insights into protein structure-function relationships and the mechanisms of diseases associated with protein misfolding and aggregation, such as Alzheimer's and Parkinson's diseases.[1] The process of protein denaturation also widely exists in normal life. For example, the structure and function of some mononuclear metalloenzymes are usually dependent on metal atoms. These enzymes are highly sensitive to metal-catalyzed Fenton reaction, which oxidizes the side chains of the proteins and lead to enzyme inactivation.[2] In addition, protein unfolding is the first step in protein sequencing. Studying the denaturation process of protein unfolding is also beneficial to the development of protein sequencing techniques.[3, 4] Overall, protein denaturation plays an important role in biological function and impacts both medical and health.[5-8]

Various techniques can be employed to monitor the changes in protein conformation and function that occur during denaturation, including Ultraviolet–visible spectroscopy,[9] Circular dichroism spectroscopy (CD),[10] dynamic light scattering[11] and mass spectrometry.[12] However, these bulk or ensemble technologies provide average rather than heterogeneous characteristics of the protein. Moreover, these methods cannot reveal the dynamic transformation processes at the single-molecule level. To address this limitation, single molecule techniques such as single molecule fluorescence[13] and single molecular force spectrometry[14, 15] are used in the study of protein denaturation. However,

View Article Online
DOI: 10.1039/D4FD00117F

these techniques involve protein labeling or immobilization, which may affect the structure and function of the protein. Thus, there is a need to develop labelling-free analytical methods for protein denaturation at the single-molecule level.

Nanopore technology has garnered much attention in the field of protein analysis due to its simplicity, label-free nature and high sensitivity.[16, 17] Some research have reported studies of protein denaturation using nanopores,[18, 19] but the rapid translocation duration prevents detailed structural information about the protein and real-time mechanistic studies of the denaturation process of individual proteins. Therefore, trapping individual proteins to study structural changes induced by denaturants is an attractive strategy. Recently, nanopore electro-osmotic flow based on the DNA-origami sphere has been used to trap single proteins and study protein dynamics.[20] However, biological components, such as DNA, are challenging for protein denaturation under extreme conditions. The high stability of inorganic material, such as silicon nitride trapping structure, allows for long-term capture of single proteins and provides insights into protein structure during denaturation.[21] However, proteins have a high tendency to stick to the SiN_x membrane, necessitating a reduction of non-specific adsorption on SiN_x nanonets. In this study, the nanonets were coated with polyethylene glycol to reduce non-specific adsorption for long-term analysis of single proteins. Using guanidine hydrochloride (Gdn-HCl) and lead ions to induce protein denaturation as models, this analytical method showed a more sensitive detection capability compared to circular dichroism spectroscopy. Additionally, it was clearly observed that the protein denaturation process exhibited a significant dependence on the concentration of the denaturant.

Experimental

Reagents and materials

Guanidine hydrochloride (Gdn-HCl, 99.5%), Lead chloride ($PbCl_2$, >99%), Tris (hydroxymethyl) aminomethane, Tris, 99%) and Ethylenediaminetetraacetic acid disodium salt (EDTA-2Na, 98%) and polyethylene glycol (PEG, aberage Mn 200) were purchased from Adamas Reagent Co., LTD. Potassium chloride (KCl), hydrochloric acid (HCl), ethanol (CH_3CH_2OH), hydrogen peroxide (H_2O_2) and sulfuric acid (H_2SO_4) were purchased from Sinopsin Chemical Reagent Co., LTD. (Shanghai, China). All chemicals were used as received without further purification. Ovalbumin (44.5 kDa) from chicken egg white was obtained from Sigma-Aldrich (Shanghai, China). Ovalbumin has 385 amino acid residues with a disulfide bond and four free sulfhydryl groups at its center. These residues intertwine and fold to form a highly stable secondary structure. Ultrapure water (18.2 MΩ cm) used in the experiments was obtained by a Standard arium® mini plus water purification system (Goettingen, Germany). The buffer solution was filtered through a 0.22 μm Millipore filter before use.

Nanonets fabrication and PEG coating

SiN_x chips with 20×20 μm 20 nm-thick membranes were fabricated as previously described by Dekker.[22] The 15-20 nm SiN_x nanopore was drilled using TEM (JEM-F200, 200 keV). The transformation from nanopores to nanonets, and modification with PEG were performed simultaneously. For detail the prepared nanopores were cleaned with piranha solution (80 ℃) for 30 min to obtain a hydrophilic surface. Afterward, the nanopores were placed in 1% (v/v) PEG ethanol solution, irradiated with xenon lamp (PLS-FX300HU, Perfect Light) equipped with a 550 nm

bandpass filter for 3 h. The chips were removed from the solution, rinsed with ethanol, and finally put them in the oven (60 ℃) to dry for 1 h.

View Article Online
DOI: 10.1039/D4FD00117F

SiN_x nanonets for single protein denaturation analysis

The SiN_x chips were treated with oxygen plasma for about 5 min to enhance the pore wettability and then mounted on a home-made flow cell with *cis* and *trans* chambers. The buffer solution (1 M KCl, 10 mM Tris-HCl, 1 mM EDTA, pH 7.5) was added to the two chambers. A pair of Ag/AgCl electrodes were employed to introduce a bias potential to the nanonets. The whole device was placed in the Faraday cage. Ovalbumin at a final concentration of 4 μg/ml was added to the *cis* end. All ionic currents were measured by a patch clamp amplifier (Axopatch 200B, Molecular Devices) combined with a digital-to-analog converter (Axon Digidata 1550B, Molecular Devices). Data were recorded using Clampex 10.7 (Molecular Devices) at a sampling frequency of 100 kHz using a 10 kHz four-pole Bessel low-pass filter.

Results and discussion

As shown in Fig. 1a, PEG-modified silicon nitride nanonets were obtained by shrinking the TEM-prepared nanopores in PEG solution under irradiation. After light treatment, the SiN_x nanopore was transformed into nanonet (Fig. 1b, c), and the structure of the nanonet is not destroyed by heat (Fig. 1d). The ionic conductance measurements and the electrical noise properties of the SiN_x nanopores and the PEG deposited nanonets were displayed in Fig. 2a, b. Both bare pore (with a diameter of ~15 nm) and PEG coated nanonets exhibit an ohmic behavior in the voltage range of −200mV to 200mV with ionic conductance of 102.1nS and 89.5nS, respectively. The 1/f (≲100 Hz) noise and white noise (~0.1–2 kHz) of PEG coated nanonets were larger than that of SiN_x nanopore. The inhomogeneities of surface PEG layer and nanonets resulted in fluctuations of the number and mobility of charge carriers. The dielectric (~2–10 kHz) and capacitive noise (>10 kHz) of PEG coated nanonets and SiN_x nanopore exhibited no significant difference, which was related to the capacitance of chip.

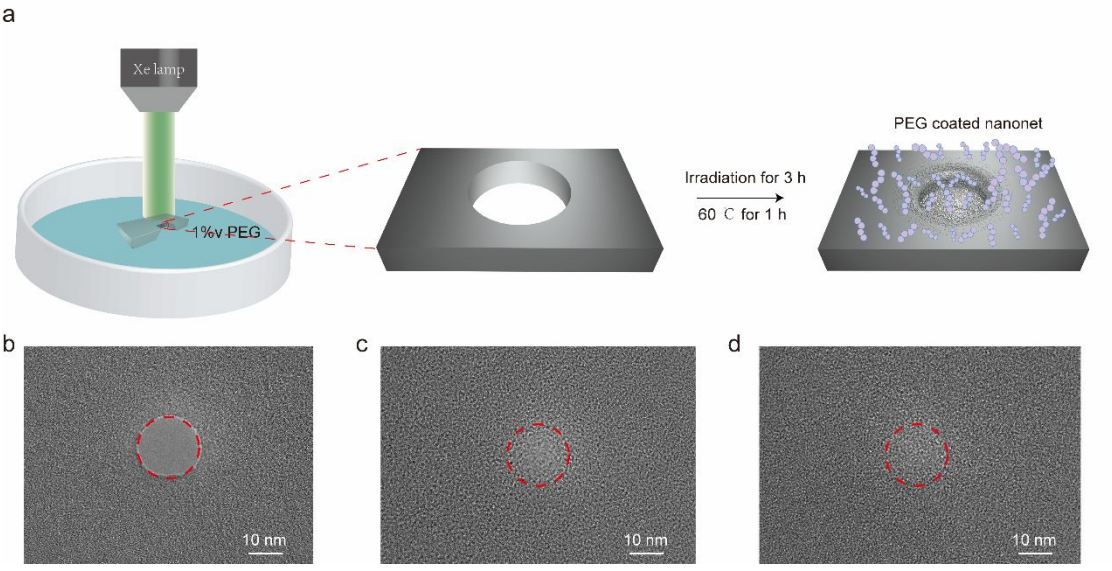

Fig.1 Preparation and modification of SiN_x nanonets. (a) Schematic diagram of the conversion of SiN_x nanopores into PEG-coated nanonets by irradiation. (b-d) Transmission electron microscopy images of SiN_x nanopore (b), PEG-coated nanonets before (c) and after (d) drying at 60 ℃. Scale

bar: 10 nm.

To check the effectiveness of the antifouling properties of PEG coated SiN_x nanonets, ovalbumin trapping and collision experiments were performed. Non-specific adsorption of proteins was encountered when SiN_x nanonets were used to analyses ovalbumin (Fig. S1)[23]. As the silanol groups on the surface of silicon-based materials are easily bound to the strong electronegative atoms inside the proteins,[24] irreversible adsorption between the nanonet and the protein easily occurs. PEG has two optional hydrogen donors, which can act as a silanol coupling agent and connect to the SiN_x surface through hydrogen bonding force to shield silanol groups and form a buffer layer between the protein molecules and the nanonet to further avoid the non-specific adsorption of proteins. A large number of collision signals were observed at 300 mV voltage and the ovalbumin did not block the nanonet,[25] which is a significant improvement compared to uncoated nanopores (Fig. 2c). The ovalbumin can be captured and released multiple times by electroosmotic flow by adjusting the voltage (Fig. 2d), indicating that they are not specifically attached to the nanonets.

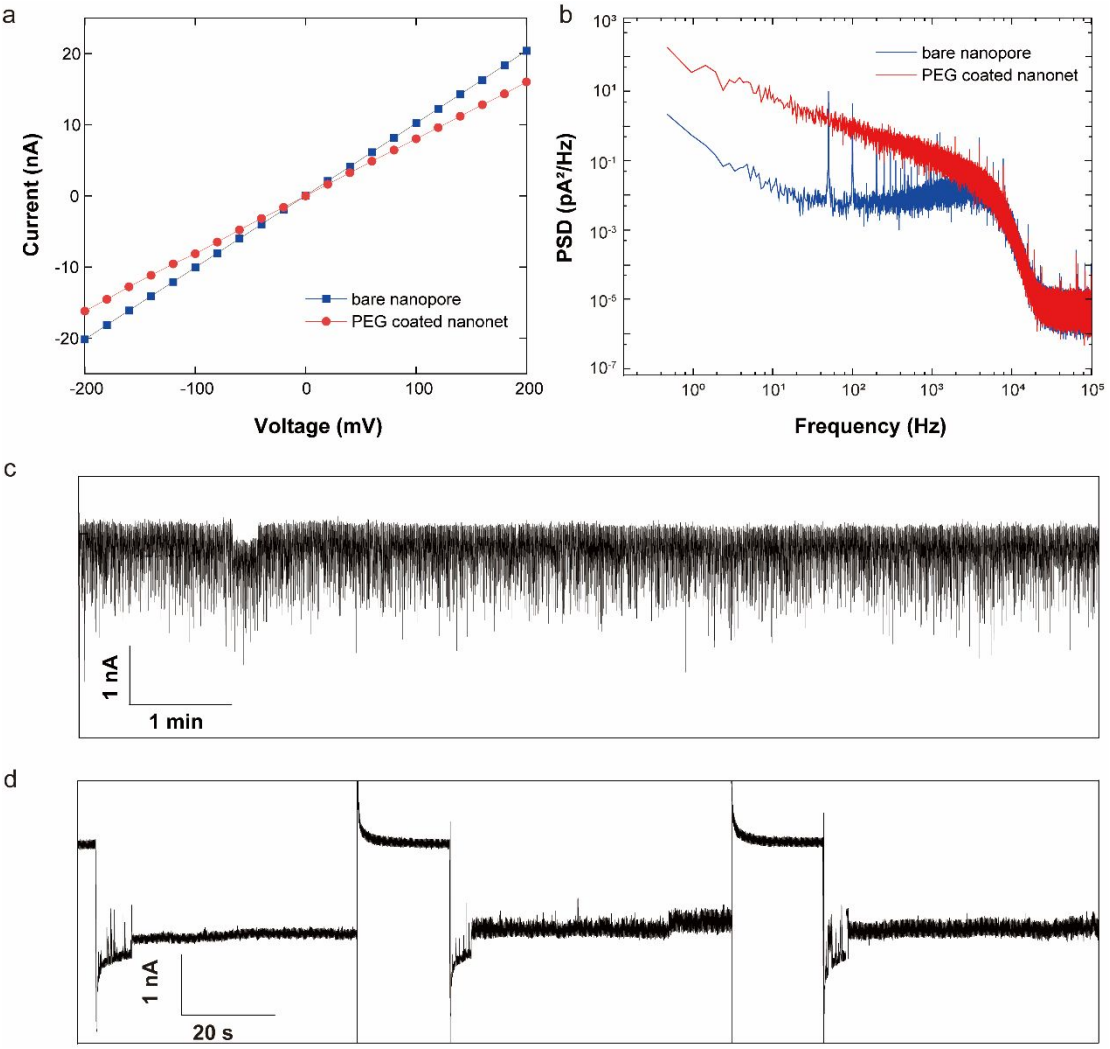

Fig.2 Effect of PEG modification (a) I-V curve of SiN_x nanopores (blue) and PEG- modified SiN_x nanonets (red). (b) Power Spectrum Densities (PSDs) of SiN_x nanopores (blue) and PEG-modified SiN_x nanonets (red) at 100 mV in 1–100 kHz frequency range. (c) Typical current signals of ovalbumin detected by PEG-coated SiN_x nanonets at 300 mV. (d) Current traces of PEG-coated SiN_x for capture and release of ovalbumin.

View Article Online
DOI: 10.1039/D4FD00117F

To characterize the denaturation process of individual ovalbumin, it was necessary to trap it using electroosmotic flow. The suitable voltage is critical for capturing ovalbumin. At low voltages, the collision signals and some unstable short-term capture signals were mainly observed (Fig. S2). A high voltage tended to capture multiple proteins and squeeze the proteins resulting in structural changes. After a single ovalbumin was captured, different concentrations Gdn-HCl were added to the *cis* end (Fig. 3a). As shown in Fig. 3c, the ionic current rapidly decreased by about 2 nA in a few seconds (~ 4 s) after the addition of 0.3 M Gdn-HCl, indicating that ovalbumin undergoes rapid denaturation when exposed to this concentration of Gdn-HCl. In contrast, the same concentration of Gdn-HCl slightly increased the ionic current when ovalbumin is not present (Fig. S3). In addition, the denaturation process took about 25 s and 5 min at Gdn-HCl concentrations of 0.2 M and 0.1 M, respectively (Fig. S4). This suggests that the rate of ovalbumin denaturation is concentration-dependent. At high concentrations of denaturants, the denaturation process of proteins occurs almost immediately. This may be due to the fact that it takes longer time for lower concentration of Gdn-HCl to diffuse and reach the denaturation threshold concentration for individual protein. In the early stages of denaturation, Gdn-HCl disrupts hydrogen bonds within the protein structure, leading to the unfolding of the protein, which increases its volume and finally decreases the ionic current.[26, 27] It was also observed that the current in the denaturation process recovered occasionally, demonstrating that some self-protection mechanism also exists in the protein during the denaturation process (Fig. 3d). This resistance phenomenon is more pronounced at lower denaturant concentrations, leading to prolonged denaturation times. The denaturant further reacts with the free -SH groups within the protein, disrupting the secondary structure and exposing the hydrophilic groups of the protein completely, which may induce significant protein aggregation and recombination.[28] The degeneration of ovalbumin induced by Gdn-HCl was also investigated by CD spectroscopy (Fig. S5). The amount of α-helices (208 nm and 222 nm) in the structure of ovalbumin reduced after treatment of ovalbumin with 0.3 M Gdn-HCl for 12 hours. However, the CD spectra of Gdn-HCl at a concentration of 0.1 M showed no significant change. These results suggest that the analysis nanonet is more sensitive for denaturation processes.

The renaturation of ovalbumin was further investigated by dilution method (Fig. 3b). As shown in Fig. 3e, after continuous dilution of Gdn-HCl, the ionic current slowly and eventually returned to the original level. This indicates that the denatured protein solution is gradually diluted to reduce the concentration of the denaturant, allowing the protein to refold to its native state. Thus the denaturation of Gdn-HCl is a reversible process.

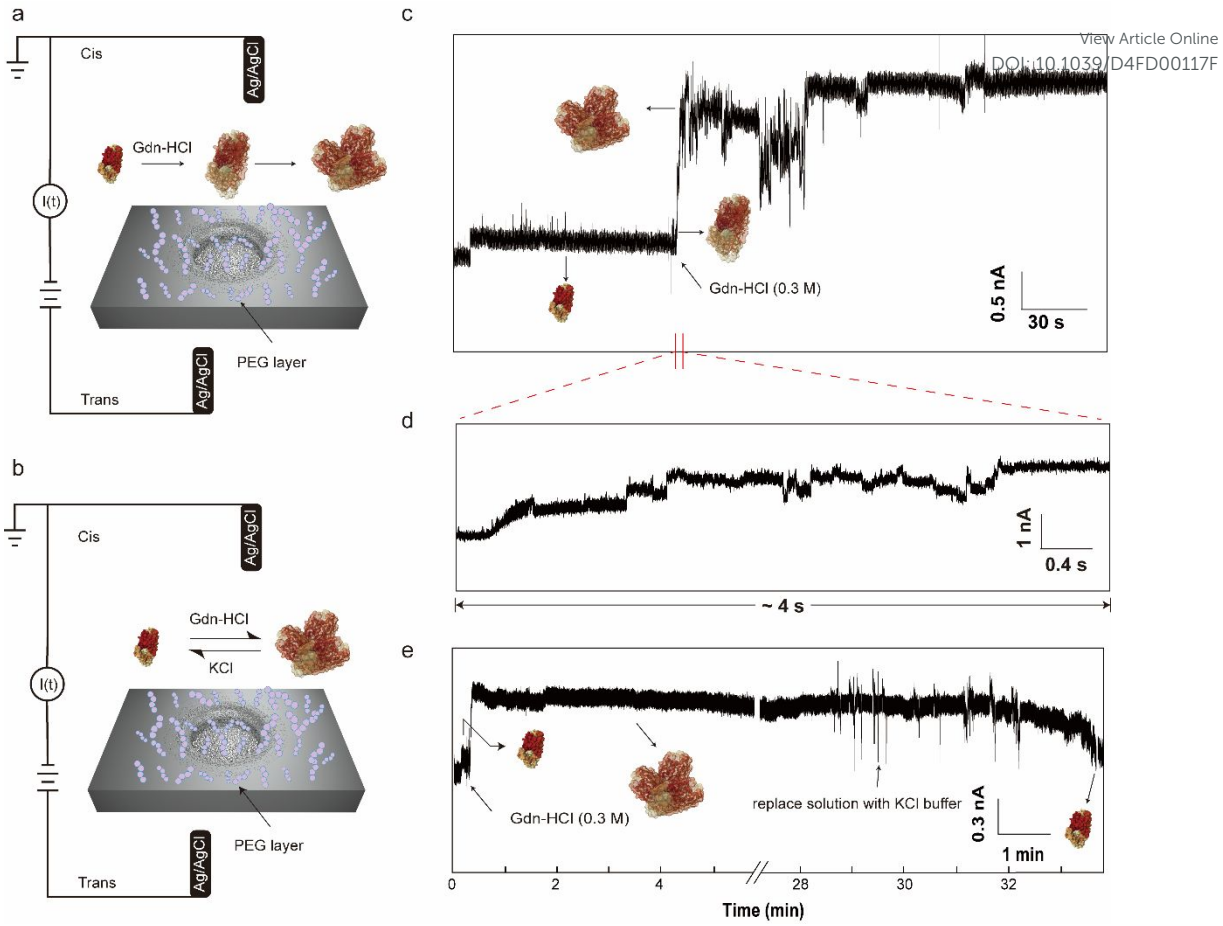

Fig.3 Reversible degeneration of ovalbumin by Gdn-HCl. (a) Schematic diagram of ovalbumin capture by PEG-coated nanonets and denaturation of ovalbumin by Gdn-HCl. (b) Schematic diagram of denaturation and renaturation of ovalbumin. (c) Current records of ovalbumin capture by electroosmotic flow and subsequent changes of ion flow with time in the presence of Gdn-HCl. The data was collected at -300 mV and the initial diameter of the nanopore was about 15 nm. (d) a detailed enlarged view of the denaturation phase in (c). (e) Current records of denaturation and renaturation of ovalbumin under Gdn-HCl. The data was collected at -200 mV and the diameter of the nanonet was about 17 nm.

To further demonstrate the universality of this method for studying protein denaturation, the denaturation of ovalbumin caused by Pb^{2+} was studied using PEG-coated nanonets (Fig. 4a). In order to prevent the interference of EDTA in the original buffer solution on the chelation of Pb^{2+}, EDTA was removed from the buffer solution. After the addition of 2.64 mM Pb^{2+}, the ionic current steadily decreases (Fig. 4b), which differs from 0.3 M Gdn-HCl. The denaturation process of Gdn-HCl was completed in 5 s, while the denaturation process of Pb^{2+} lasted more than 10 min. Similar structure changes could be observed for Pb^{2+}, including unfolding and aggregation, although the its concentration of Pb^{2+} is two orders of magnitude lower than Gdn-HCl. This may be related to the fact that Pb^{2+} have a high affinity for sulfur-containing amino acids like cysteine and methionine, disrupting disulfide bridges that are crucial for maintaining protein structure.

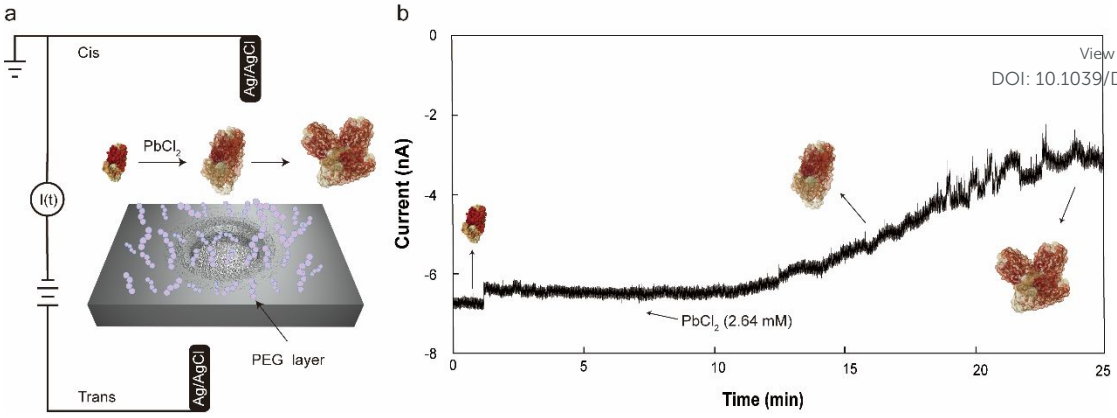

Fig.4 Degeneration of ovalbumin by $PbCl_2$. (a) Schematic diagram of ovalbumin capture by PEG-coated nanonets and denaturation of ovalbumin by $PbCl_2$. (b) Current records of ovalbumin capture by electroosmotic flow, and changes of ionic current with time in the presence of $PbCl_2$. The data was collected at -200 mV.

Conclusions

In this paper, we have solved the problem of non-specific adsorption of protein with SiN_x nanonet by using PEG functionalization, and studied the structural changes of single ovalbumin under the action of two denaturators, Gdn-HCl and Pb^{2+}. The changes of ion current show that the denaturation process induced by both denaturators is accompanied by protein unfolding and protein aggregation. The renaturation process of ovalbumin under the action of Gdn-HCl was also studied. The results showed that the denatured protein could return to the normal folded structure by diluting the denaturant concentration. In further work, spectroscopy such as surface-enhanced Raman and Infrared can be combined with nanonets to provide an additional dimension of information on the understanding of various amino acid residues in secondary and primary structures during protein conformational processes.

Conflicts of interest

The authors declare no competing interests.

Acknowledgements

The authors would like to acknowledge the support of the Center for Nanoscience and Nanotechnology at Wuhan University. Y.Z. acknowledges the financial support from National Key R&D Program of China (2021YFA0909900), the Fundamental Research Funds for Central Universities (No. 2042024kf0012), and the start-up funds of Wuhan University. B.H. acknowledges the financial support from China Postdoctoral Science Foundation (No. 2023M742689, GZB20230545).

References

1. B. N. Dugger and D. W. Dickson, *Cold Spring Harbor Perspect. Biol.*, 2017, **9**, 28-35.
2. J. A. Lemire, J. J. Harrison and R. J. Turner, *Nat. Rev. Microbiol.*, 2013, **11**, 371-384.
3. R. Strack, *Nat. Methods*, 2023, **20**, 1868-1868.
4. L. Yu, X. Kang, F. Li, B. Mehrafrooz, A. Makhamreh, A. Fallahi, J. C. Foster, A. Aksimentiev,

M. Chen and M. Wanunu, *Nat. Biotechnol.*, 2023, **41**, 1130-1139.

5. Y. Wang, D. Zheng, Q. Tan, M. X. Wang and L.-Q. Gu, *Nat. Nanotechnol.*, 2011, **6**, 668-674.
6. N. S. Galenkamp, M. Soskine, J. Hermans, C. Wloka and G. Maglia, *Nat. Commun.*, 2018, **9**, 4085.
7. N. Burck, T. Gilboa, A. Gadi, M. Patkin Nehrer, R. J. Schneider and A. Meller, *Clin. Chem.*, 2021, **67**, 753-762.
8. Y. Wang, K. Tian, R. Shi, A. Gu, M. Pennella, L. Alberts, K. S. Gates, G. Li, H. Fan, M. X. Wang and L.-Q. Gu, *ACS Sens.*, 2017, **2**, 975-981.
9. N. Poklar and G. Vesnaver, *J. Chem. Educ.*, 2000, **77**, 380.
10. S. K. Haq and R. H. Khan, *Int. J. Biol. Macromol.*, 2005, **35**, 111-116.
11. A. S. Eissa, *Food Hydrocolloids*, 2019, **87**, 97-100.
12. M. Mathay, A. Keller and J. E. Bruce, *Anal. Chem.*, 2023, **95**, 9432-9436.
13. I. M. Vedel, A. Papagiannoula, S. Naudi-Fabra and S. Milles, *Curr. Opin. Struct. Biol.*, 2023, **82**, 102659.
14. N. A. Barinov, A. D. Protopopova, E. V. Dubrovin and D. V. Klinov, *"Colloids Surf., B"*, 2018, **167**, 370-376.
15. P. N. Nirmalraj, M. D. Rossell, W. Dachraoui, D. Thompson and M. Mayer, *ACS Appl. Mater. Interfaces*, 2023, **15**, 48015-48026.
16. L. Xue, H. Yamazaki, R. Ren, M. Wanunu, A. P. Ivanov and J. B. Edel, *Nat. Rev. Mater.*, 2020, **5**, 931-951.
17. Y.-L. Ying, Z.-L. Hu, S. Zhang, Y. Qing, A. Fragasso, G. Maglia, A. Meller, H. Bayley, C. Dekker and Y.-T. Long, *Nat. Nanotechnol.*, 2022, **17**, 1136-1146.
18. H. Sun, C. Yao, K. You, C. Chen, S. Liu and Z. Xu, *Anal. Chim. Acta*, 2023, **1243**, 340803.
19. G. Oukhaled, J. Mathé, A. L. Biance, L. Bacri, J. M. Betton, D. Lairez, J. Pelta and L. Auvray, *Phys. Rev. Lett.*, 2007, **98**, 158101.
20. S. Schmid, P. Stömmer, H. Dietz and C. Dekker, *Nat. Nanotechnol.*, 2021, **16**, 1244-1250.
21. J. Li, B. Huang, Y. Wang, A. Li, Y. Wang, Y. Pan, J. Chai, Z. Liu and Y. Zhai, *Adv. Mater.*, 2023, **35**, 2210342.
22. X. J. A. Janssen, M. P. Jonsson, C. Plesa, G. V. Soni, C. Dekker and N. H. Dekker, *Nanotechnology*, 2012, **23**, 1136-1146.
23. D. J. Niedzwiecki, J. Grazul and L. Movileanu, *J. Am. Chem. Soc.*, 2010, **132**, 10816-10822.
24. Z. Tang, B. Lu, Q. Zhao, J. Wang, K. Luo and D. Yu, *Small*, 2014, **10**, 4332-4339.
25. B. Cressiot, A. Oukhaled, G. Patriarche, M. Pastoriza-Gallego, J.-M. Betton, L. Auvray, M. Muthukumar, L. Bacri and J. Pelta, *ACS Nano*, 2012, **6**, 6236-6243.
26. M. Zemser, M. Friedman, J. Katzhendler, L. L. Greene, A. Minsky and S. Gorinstein, *J. Protein Chem.*, 1994, **13**, 261-274.
27. E. R. Stadtman and R. L. Levine, *Amino Acids*, 2003, **25**, 207-218.
28. J. Tyedmers, A. Mogk and B. Bukau, *Nat. Rev. Mol. Cell Biol.*, 2010, **11**, 777-788.

Data Availability Statement

All data supporting the findings of this study are available within the paper and its Supplementary Information.

View Article Online
DOI: 10.1039/D4FD00117F